Dynamics of a curved Fermi-Pasta-Ulam chain: Effects of geometry, long-range interaction, and nonlinear dispersion

Ranja Sarkar and Bishwajyoti Dey
Department of Physics, University of Pune, Pune-411007, India
(Received 14 December 2006; revised manuscript received 30 May 2007; published 17 July 2007)

We study the dynamics of the bent Fermi-Pasta-Ulam (FPU) chain, incorporating the complicated effects of geometry, long-range interactions, as well as nonlinear dispersion. Within the rotating wave approximation, we obtain several exact discrete breather (DB) solutions, such as the odd-parity and even-parity discrete breathers, compactlike discrete breathers and moving discrete breathers for various geometries of the chain. In presence of long-range nonlinear dispersive interactions, we show that DBs exist in the discrete curved lattice for next-nearest-neighbor interactions as well. For all neighbors interactions, we treat the problem in the long-wavelength (continuum) and weakly nonlinear limit of the system and obtain exact static breather solutions and large-amplitude, traveling kink-soliton solutions. The curved FPU chain also admits finite amplitude discrete nonlinear sinusoidal wave solutions with short commensurate as well as incommensurate wavelengths. The usefulness of these solutions for energy localization and transport in various physical systems are discussed.

DOI: 10.1103/PhysRevE.76.016605 PACS number(s): 36.20.−r, 87.15.−v, 63.20.Ry, 63.20.Pw

I. INTRODUCTION

Intrinsic localized modes (ILMs) or discrete breathers (DBs) which are typical excitations in periodic lattices of weakly coupled nonlinear oscillators have been extensively discussed during the past several years. ILMs have been observed in various physical systems ranging from lattice vibrations in crystals [1] and magnetic solids [2], to microengineered structures including Josephson junctions [3], optical wave-guide arrays [4], photonic crystals [5], and more recently in a layered crystal insulator at room temperature [6]. The importance of these nonlinear excitations has been emphasized in the modeling of biopolymers and conducting polymers and it is suggested that these excitations may provide a possible physical mechanism for energy transport and storage as well as for structural properties of biopolymers [7], charge transport in conducting polymers [8], and more recently, creation of magnetic metamaterials with domains of opposite sign magnetic response [9]. It is also suggested that ILMs may play crucial roles in the trapping of energy and other dynamical properties [10], such as melting transitions in solids, materials in the glassy state, observed dark lines or a "tracks" forming process along a crystal direction in white mica [11], folding in the polypeptide chain and in the targeted breaking of chemical bonds [12].

Recent advances in nanotechnology have made it possible to fabricate various low-dimensional systems with complicated geometry, such as photonic crystals with embedded defects, wave guide with wave-guide bends which are the perfect grounds for creation and observation of DBs or ILMs, quantum dots, magnetic nanodisks, etc. Observed properties of these systems depend on their geometry. For example, the electronic properties of a carbon nanotube depend on its chirality. Recent nanoparticle research has created shape-shifting polymers, a novel material that changes shape in response to a suitable magnetic field without having to change the ambient temperature and has great potential applications in noninvasive drug delivery, remotely controlled instruments, and "smart" implant, etc. [13]. Likewise, the biological systems or the biological macromolecules, such as proteins, DNA, etc. have very complex structures and their structure is crucial for their functionality. Besides geometry, long-range interactions also play a crucial role in the functioning of such systems. The charged groups in molecular chains and DNA molecules interact through long-range dipole-dipole interaction. Similarly, when a crystal surface is bombarded with heavy ions, the on-site potential and long-range interaction between atoms can influence the disposal of energy in the lattice by creation of energetic, mobile, highly localized lattice excitations that can propagate great distances (observed $\sim 10^7$ unit cells in insulating muscovite crystal [6]) in atomic chain directions. Therefore, in order to address the above-mentioned complex phenomena, one needs to study models that incorporate the more complicated effects of structure or geometry of the physical systems, long-range interactions as well as nonlinear dispersion.

Analytical studies of nonlinear lattice problems are limited to approximate solutions of the corresponding discrete nonlinear dynamical equations. Lattice Green's function techniques have been used to obtain analytically approximate DB solutions [14]. Another approximate analytical method usually used to find DB solutions is to solve the corresponding continuum equations in the long-wavelength limit [15,16]. Alternately, numerical simulations of the discrete equations of motion of the nonlinear lattices in higher spatial dimensions have been used to obtain information regarding the DB dynamics in various systems [17] including the dynamics of two-dimensional Josephson-junction arrays [18], the dynamics of pinned and mobile discrete breathers in two-dimensional anisotropic nonlinear Schrödinger lattices [19], observation of two-dimensional discrete solitons in optically induced nonlinear photonic lattices [4], energy localization and transport in discrete curvilinear chains [20], bubble generation in a twisted and bent DNA-like model [21], energy funneling in a bent chain of Morse oscillator with long-range coupling [22], and the existence and directional mobility of DBs along lattice directions of the two-dimensional hexagonal lattice [24].

 ©2007 The American Physical Society

In this paper, we consider a more general nonlinear lattice problem. We include the essential anharmonicity by considering nearest-neighbor interaction potential as Fermi-Pasta-Ulam type. In earlier similar studies, the geometry of the chain was restricted to a parabola or a wedge shape, i.e., a fixed set of angles between bond vectors at different lattice sites or two straight segments of the chain joined by a bent section [20–22]. We remove these constraint conditions on the dynamics of the chain and consider both the radial coordinates as well as the angular coordinates of the position vectors as dynamical variables. Moreover, we consider both the cases when the arbitrary shape of the chain is time independent as well as time dependent. We further generalize the problem by including long-range interactions to examine the interplay of long-range interaction, nonlinear dispersion, and geometry on the dynamics of the nonlinear lattice. Accordingly, we study analytically the dynamics of the curved FPU chain of arbitrary shape in the presence of long-range nonlinear dispersive interactions with power dependence r^{-s} on the distance. We obtain exact static and traveling discrete breather solutions and study the effects of geometry of the chain, long-range interactions, and nonlinear dispersion on the properties of these solutions. We show that besides the DBs, the system supports compactlike DB solutions for a certain geometry of the chain. We further show that finite amplitude, traveling nonlinear sinusoidal waves with short commensurate as well as incommensurate wavelengths and in general, amplitude-dependent frequencies are exact solutions of the curved FPU chain.

The plan of the paper is as follows: in Sec. II we derive the equations of motion governing the system. Section III is devoted to static ILMs or DBs, both of odd-parity and even-parity mode and also compactlike DBs, while in Sec. IV we consider the moving DBs. In Sec. V we study the dynamics of the curved FPU chain in the presence of long-range nonlinear dispersive interactions. In Sec. VI we look for the exact finite amplitude, traveling nonlinear sinusoidal wave (NSW) solutions with short and commensurate as well as incommensurate wavelengths of the curved FPU chain and finally we conclude in Sec. VII.

II. EQUATIONS OF MOTION

We consider a simple model of a polymer chain consisting of N units, each of mass m, labeled by index n and denoted by x_n, y_n the longitudinal and transverse positions with respect to a two-dimensional (2D) Cartesian coordinate system. Such a chain embedded in a plane has a direct physical meaning and can describe, for example, molecular crystals and shape-shifting polymers, biophysical systems, etc. The Hamiltonian is

$$H = \sum_n \left(\frac{\dot{x}_n^2}{2} + \frac{\dot{y}_n^2}{2} + V(d_n) \right), \tag{1}$$

where we have considered unit mass of each particle and d_n is the distance between the adjacent mass points given by

$$d_n = [(x_n - x_{n-1})^2 + (y_n - y_{n-1})^2]^{1/2}. \tag{2}$$

We model the essential anharmonicity in the system, apart from the geometric one entering through d_n, of the FPU type viz.,

$$V(d_n) = K_2 \frac{(d_n - a)^2}{2} + K_4 \frac{(d_n - a)^4}{4}, \tag{3}$$

where a is the equilibrium distance between particles in the chain, K_2 and K_4 are strengths of linear and nonlinear forces. The equations of motion are given by

$$\ddot{x}_n = \frac{x_n - x_{n-1}}{d_n} f_n - \frac{x_{n+1} - x_n}{d_{n+1}} f_{n+1}, \tag{4}$$

$$\ddot{y}_n = \frac{y_n - y_{n-1}}{d_n} f_n - \frac{y_{n+1} - y_n}{d_{n+1}} f_{n+1}, \tag{5}$$

where $f_n = -\frac{dV}{dd_n}$. By introducing relative distances ξ_n, ρ_n normalized to the equilibrium distance a and a complex plane representation defined through

$$\xi_n = \frac{x_n - x_{n-1}}{a}, \quad \rho_n = \frac{y_n - y_{n-1}}{a}, \tag{6}$$

$$z_n = \xi_n + i\rho_n, \tag{7}$$

we can write the equations of motion in a compact form as

$$\ddot{z}_n = R_{n+1} + R_{n-1} - 2R_n, \tag{8}$$

where

$$R_n = \frac{z_n}{|z_n|}[(|z_n| - 1) + \gamma(|z_n| - 1)^3]. \tag{9}$$

Here time has been normalized to $\sqrt{K_2}t$ and $\gamma = \frac{K_4 a^2}{K_2}$ denote the anharmonicity parameter. Since we are interested in studying the dynamics of an arbitrary shaped chain, it is useful to transform to polar coordinate representation $z_n = r_n(t)e^{i\theta_n(t)}$ and on further using $\tau_n(t) = [r_n(t) - 1]$ we obtain two coupled difference-differential equations from the real and imaginary parts, respectively, as

$$\ddot{\tau}_n - (\tau_n + 1)\dot{\theta}_n^2 = g_{n+1}\cos(\theta_{n+1} - \theta_n) + g_{n-1}\cos(\theta_{n-1} - \theta_n) - 2g_n, \tag{10}$$

$$(\tau_n + 1)\ddot{\theta}_n + 2\dot{\tau}_n\dot{\theta}_n = g_{n+1}\sin(\theta_{n+1} - \theta_n) + g_{n-1}\sin(\theta_{n-1} - \theta_n), \tag{11}$$

where $g_n = \tau_n + \gamma\tau_n^3$. The local variables (τ_n, θ_n) represent the local relative deviation of two adjacent masses in the chain normalized with respect to the lattice spacing a and its angular deviation with respect to a given axis, respectively. When all local angles are zero, i.e., $\theta_n = 0$ for all values of n, these equations reduce to the standard one-dimensional FPU model. Under the approximation that the angular variables are time independent, i.e., $\dot{\theta}_n = 0$ for all values of n, Eq. (10) reduces to

$$\ddot{\tau}_n = g_{n+1}\cos(\theta_{n+1}-\theta_n) + g_{n-1}\cos(\theta_{n-1}-\theta_n) - 2g_n. \tag{12}$$

Equation (12) is the dynamical equation studied by Tsironis *et al.* [Eq. (8) in [20]] numerically for a simple hairpin geometry of the polymer chain. They considered the second equation (11), which for $\dot{\theta}_n=0$ reduces to

$$0 = g_{n+1}\sin(\theta_{n+1}-\theta_n) + g_{n-1}\sin(\theta_{n-1}-\theta_n) \tag{13}$$

as a constraint condition. For simplicity they ignored the second equation, Eq. (13), completely and accordingly studied the constrained dynamics of the system. We remove these constraint conditions used in [20] and consider both the coupled equations (10) and (11) for the dynamics. We further remove the fixed curvature condition assumed in earlier studies as mentioned above and consider arbitrary shapes of the chain. We consider the cases when all local angles θ_n are time independent as well as time dependent. This enables us to study the dynamics of the arbitrary shaped chain both fixed as well as changing in time.

III. STATIC DISCRETE BREATHERS

Let us first consider the case where θ_n are time independent, i.e., $\dot{\theta}_n=0$ for all n. Before considering the dynamics of the coupled equations (10) and (11), we study the dynamics of Eq. (12) as a special case. As mentioned above, Tsironis *et al.* studied Eq. (12) numerically to look for propagating DBs for a simple hairpin geometry of the chain. We show analytically that the same equation also supports several exact static localized solutions, such as DBs with odd and even parity and compactlike DBs for different geometries of the chain. We use the ansatz for the DB solutions

$$\tau_n = \phi_n \cos(\omega t). \tag{14}$$

We define the geometry of the chain as

$$\cos(\theta_{n+1}-\theta_n) = \frac{\mu}{(1+\gamma_1\phi_{n+1}^2)},$$

$$\cos(\theta_{n-1}-\theta_n) = \frac{\mu}{(1+\gamma_1\phi_{n-1}^2)}, \tag{15}$$

where the parameter μ characterizes the shape of the chain and $\gamma_1=\frac{3}{4}\gamma$. Making use of the rotating wave approximation (RWA), which means taking into account only the first harmonics frequency contribution in the time periodic solution, we obtain the equation for ϕ_n as

$$-\omega^2\phi_n = \mu\phi_{n+1} + \mu\phi_{n-1} - 2(\phi_n + \gamma_1\phi_n^3). \tag{16}$$

A coupled harmonic problem can be separated into homogenous and inhomogenous wave solutions by utilizing the fact that for a plane wave mode the excursion of each atom is $\sim O(N^{-\frac{1}{2}})$ with N a large number, whereas the excursion of an atom for a localized mode $\sim O(1)$ with $N\sim 1$ [25]. The homogeneous plane wave solutions can be obtained by ignoring the quartic term K_4 in the potential [Eq. (3)] so that the dispersion relation simplifies to

$$\omega^2 = 2[1-\mu\cos(q)] \tag{17}$$

with real wave vector q. But when an anharmonic local mode exists, the full potential must be employed. However, far from the local mode site, the excursion in that particular mode is small, so in this region of the lattice the quartic term can again be neglected when determining the asymptotic properties of the solution. An inhomogeneous wave solution is characterized by a complex wave vector

$$q^* = q \pm iq' = (2p+1)\pi \pm iq', \tag{18}$$

where p is an integer and the sign on the second term on the right-hand side is chosen so that the solution decays with increasing distance from the local mode center. The dispersion relation for the anharmonic localized mode can be expressed in terms of the maximum plane wave frequency $\omega_m^2=2(1+\mu)$ as

$$\left(\frac{\omega}{\omega_m}\right)^2 = \frac{1+\mu\cosh(q')}{1+\mu} \tag{19}$$

We assume that far from the mode center all anharmonic localized modes must obey this expression [25].

A. Odd-parity localized modes

We let the ILM or DB be centered on the lattice site $n=0$ and look for odd-parity solutions of Eq. (16) as

$$\phi_n = \phi_{-n}, \quad \phi_n = \alpha A(-1)^n e^{-nq'} \text{ for } n>0 \tag{20}$$

with $\phi_0=\alpha$. We define a new anharmonicity parameter $\Delta=\gamma_1\alpha^2$ and write $\kappa=e^{-q'}$. For the central lattice site ($n=0$) and its nearest neighbor ($n=1$), Eq. (16), respectively, becomes

$$\left(\frac{\omega}{\omega_m}\right)^2 = \frac{1}{(1+\mu)}[(1+\Delta)+\mu A\kappa] \tag{21}$$

and

$$\left(\frac{\omega}{\omega_m}\right)^2 = \frac{1}{2(1+\mu)}\left[2(1+\Delta A^2\kappa^2) + \mu\left(\kappa+\frac{1}{A\kappa}\right)\right]. \tag{22}$$

The far-field condition [Eq. (19)] can be rewritten in terms of κ and ω_m as

$$\left(\frac{\omega}{\omega_m}\right)^2 = \frac{1}{2(1+\mu)}\left[2+\mu\left(\kappa+\frac{1}{\kappa}\right)\right]. \tag{23}$$

For given values of the anharmonicity parameter Δ and the shape parameter μ, we solve the coupled equations (21)–(23) simultaneously for κ, A, and ω^2. This gives the dependence of the relative amplitude $\left|\frac{\phi_1}{\phi_0}\right|=A\kappa$ and the local-mode frequency on the anharmonicity Δ and curvature (μ) of the chain. In Fig. 1 we plot the variation of the calculated frequencies and relative amplitudes ($A\kappa$) with the anharmonicity for two chosen curvature values. It is evident from this figure that for very small Δ values the nearest-neighbor amplitude is nearly the same as the central atom. Therefore in the small Δ limit the mode is delocalized. For large Δ the neighbors have small amplitudes with respect to that of the

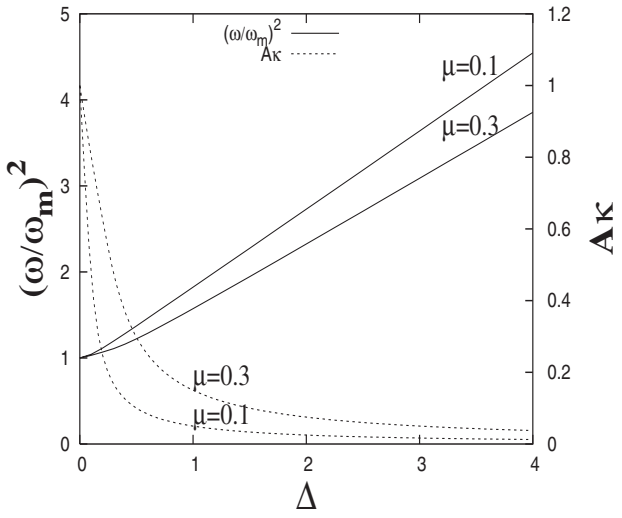

FIG. 1. Local-mode frequency and relative amplitude vs anharmonicity for the odd-parity case.

central site and therefore the DB mode becomes localized. The actual values of the relative amplitudes for different Δ depend on the curvature of the chain. For a fixed Δ value the mode becomes less localized as the μ value increases. Also, the local-mode frequency increases with increasing Δ and decreasing μ.

In Fig. 2 we plot the variation of the angular difference between the adjacent lattice sites with each lattice site n for the two μ values and in the inset we plot the change in spatial spread of the DB mode for the same. The filled circles are for larger angular differences (corresponding scale is the right-hand y axis) and the corresponding lattice displacements are shown by the filled circles in the inset. The open circles are for smaller angular differences (corresponding scale is the y axis on the left-hand side) and the corresponding lattice displacements are shown by the open circles in the inset of the figure. It is clear that as the angular differences increase (μ values decrease) the DB mode becomes more localized. It is also observed that the extent of localization does not change with the amplitude of the central lattice site (α value) and as expected, only the absolute amplitudes change. Spatially localized, temporally periodic, odd-mode breathing structures for the two different μ values are plotted in Figs. 3(a) and 3(b) which clearly shows that the localization increases as μ values decrease.

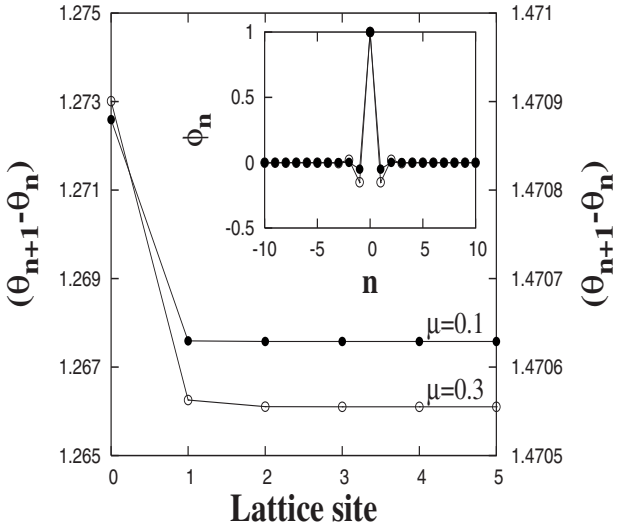

FIG. 2. Variation of the angular difference between adjacent lattice sites with lattice sites. Parameter values: Δ=1.0, α=1.0. Inset: Spatial profile of the odd-parity mode for the same parameter values.

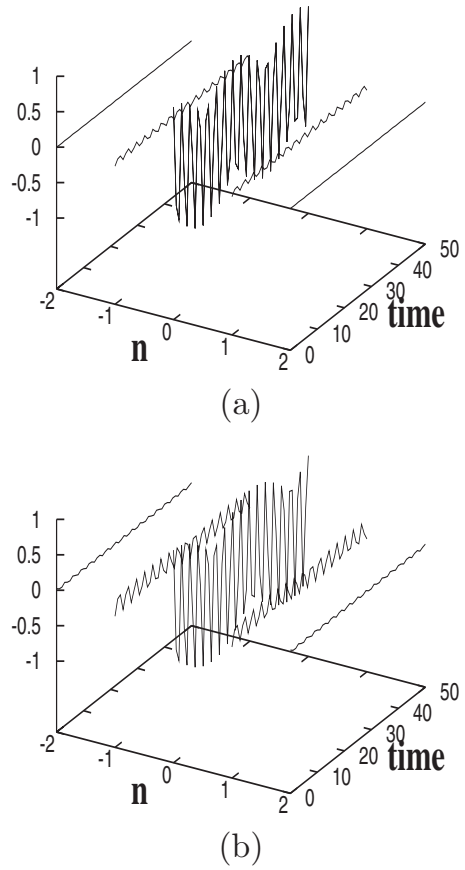

FIG. 3. Odd-parity discrete breather structure. Each solid line plots the time evolution of $\tau_n(t)$ for the lattice site n with Δ=1.0, α=1.0. Time is in units of ω_m. (a) μ=0.1; (b) μ=0.3.

B. Even-parity localized modes

We now investigate the existence of even-parity solutions of Eq. (16). In such a mode, there is no mass unit labeled n=0. The displacements of the even mode are labeled $\phi_{\pm n}$ where $n>0$ and the pattern satisfies the relation $\phi_{-n}=-\phi_n$. We take $\phi_1=\alpha$ and $\phi_n=\alpha A(-1)^{n-1}e^{-(n-1)q'}$ for $n>1$. For the n=1 lattice site, Eq. (16) yields

$$\left(\frac{\omega}{\omega_m}\right)^2=\frac{1}{2(1+\mu)}[2(1+\Delta)+\mu(1+A\kappa)]. \qquad (24)$$

For the n=2 site, the condition reduces to Eq. (22) since the nearest neighbors have the same amplitude pattern. The far-field condition, Eq. (23) remains unchanged for these modes.

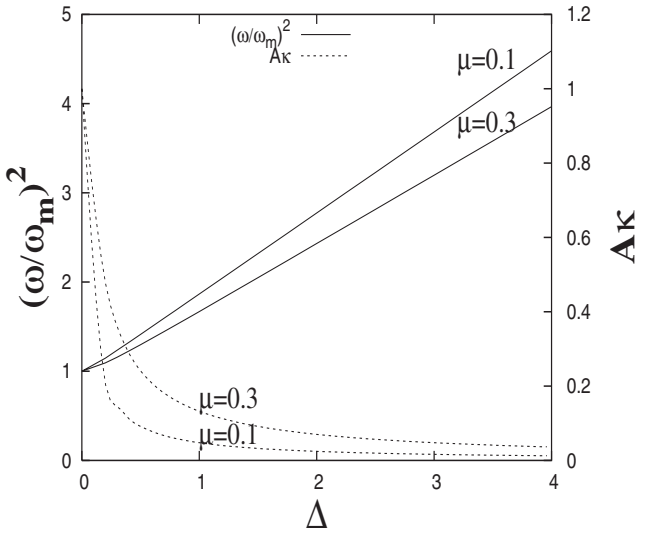

FIG. 4. Local-mode frequency and relative amplitude versus anharmonicity for the even-parity case.

For given values of the anharmonicity parameter Δ and the shape parameter μ, we solve coupled equations (22)–(24) simultaneously for κ,A, and ω^2. The dependence of the local-mode frequency and the relative amplitude $|\frac{\phi_2}{\phi_1}| = A\kappa$ of the even mode on the anharmonicity Δ for the two μ values are shown in Fig. 4. It is clear from this figure that the results are qualitatively similar to those for the odd mode presented in Fig. 1. A quantitative difference is that, for a given Δ value, the even-mode frequency is higher than the odd-mode frequency for any curvature (μ value) of the chain. Also, the relative amplitude of the odd mode is higher than that of the even mode for a given Δ value implying higher localization of the even DB mode for any chain curvature. The even-parity mode can be constructed approximately by superimposing two odd DB modes with opposite phase on next-neighbor sites [25]. Study of the even mode does not yield any extra information and therefore will not be considered further in the next sections.

C. Compactlike discrete breather modes

Most of the studies on the FPU system consider only discrete breathers as localized excitations. Although DBs can be localized practically on a single site, in most cases they have exponential spatial localized structures. However, recently it has been demonstrated that the corresponding continuum equations, the Korteweg-deVries (KdV)-like equations with nonlinear dispersion, support exact localized solutions with compact support [26]. These solutions which are termed as compactons are free of exponential tails. Unlike a soliton, a compacton is characterized by an amplitude which is independent of its width [26]. Even though discrete systems cannot support localized solutions with exact compact structure, it is now well known from the study of the lattices with nonlinear dispersive interactions that discrete lattices can support compactlike DBs [27]. Unlike DBs, the compactlike DBs are characterized by almost compact or compactlike support (superexponential) in space [28]. It has been shown that the presence of long-range interactions influences the spatial profile and properties of compactlike DBs [29]. Possible existence of compactlike DBs in nonlinear lattice systems would make them ideal for energy storage, since they would not interact until they are almost in contact with each other due to the lack of exponential tail. The resulting increase in their lifetime would be important in applications such as energy transport, signal processing, and communications.

In a recent paper [30] we have shown that for time independent θ_n the coupled equations (12) and (13) support exact static discrete compactlike DBs and for time dependent θ_n, the coupled equations [Eq. (10) and (11)] support discrete traveling compactlike DBs for different geometries of the chain. Here we report a compactlike DB solution to Eq. (12) for yet another chain geometry. For this we use the ansatz

$$\tau_n = A\phi_n \cos(\omega t),$$

where A is the amplitude of the compactlike DB. We consider the shape of the chain as

$$\cos(\theta_{n+1} - \theta_n) = \mu\phi_{n+1}^2,$$

$$\cos(\theta_{n-1} - \theta_n) = \mu\phi_{n-1}^2, \tag{25}$$

where μ is the parameter describing the shape. The corresponding equation of motion thus derived from Eq. (12) using RWA is

$$(2-\omega^2)\phi_n + 2\gamma_1 A^2 \phi_n^3 = \mu[(\phi_{n+1}^3 + \phi_{n-1}^3) + \gamma_1 A^2(\phi_{n+1}^5 + \phi_{n-1}^5)]. \tag{26}$$

This equation supports solutions with compactlike spatial profile,

$$\phi_n = \cos[B(n-n_0)] \quad \text{for } |n-n_0| < \frac{\pi}{2B} = 0 \quad \text{otherwise.} \tag{27}$$

Here n_0 denotes the mode center, and B denotes the width. Figure 5 illustrates the dependence of the breather amplitude on the anharmonicity parameter γ_1 (>0) for a particular chosen μ value. Plots are for two typical compactlike DBs of width $B=\frac{7\pi}{10}$, frequency $\omega=1.739\,97$ (curve A) and $B=\frac{\pi}{10}$, $\omega=1.353\,01$ (curve B). The amplitudes almost saturate for very large γ_1 values. The nature of the plot remains similar for other values of the shape parameter.

D. Localized mode solutions of the coupled equations of motion

Let us now take into account Eq. (13) and examine the possibility of existence of static DB modes in the coupled equations of motion, Eqs. (12) and (13). As mentioned earlier Tsironis *et al.* [20] ignored Eq. (13) completely in their study. Substituting Eq. (13) in Eq. (12) we arrive at a single differential-difference equation describing the coupled system viz.,

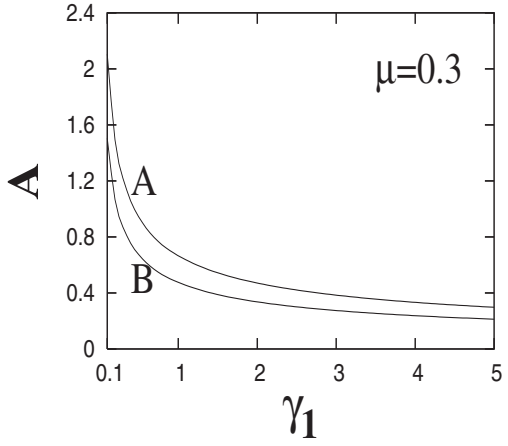

FIG. 5. Compactlike discrete breather amplitude A vs anharmonicity.

$$\ddot{\tau}_n = [g_{n+1}^2 + g_{n+1}^2 + 2g_{n+1}g_{n-1}\cos(\theta_{n+1} - \theta_{n-1})]^{1/2} - 2g_n. \tag{28}$$

Substituting the ansatz as in Eq. (14) for DB solutions in Eq. (28) and using RWA we obtain the equation

$$-\omega^2\phi_n = [(\phi_{n+1} + \gamma_1\phi_{n+1}^3)^2 + (\phi_{n-1} + \gamma_1\phi_{n-1}^3)^2 + 2\mu\phi_{n+1}\phi_{n-1}]^{1/2} - 2(\phi_n + \gamma_1\phi_n^3), \tag{29}$$

where we have defined the geometry of the chain as

$$\cos(\theta_{n+1} - \theta_{n-1}) = \frac{\mu}{[1 + \gamma_1(\phi_{n+1}^2 + \phi_{n-1}^2) + \gamma_1^2\phi_{n+1}^2\phi_{n-1}^2]}. \tag{30}$$

We now seek odd-parity DB solutions to Eq. (29) and accordingly let the mode be centered on the lattice site $n=0$. We take the displacement pattern $\phi_n = \alpha(-1)^n e^{-nq}$ for $n \geq 0$ and $\phi_n = \phi_{-n}$. Substituting ϕ_n in Eq. (29) and equating coefficients of different exponential terms to zero, we get three equations,

$$\omega^4 - 4\omega^2 = 2\mu - 4 + \left(\kappa^2 + \frac{1}{\kappa^2}\right), \tag{31}$$

$$\omega^2 = 2 - \frac{1}{2}\left(\kappa^4 + \frac{1}{\kappa^4}\right), \tag{32}$$

$$4 - \left(\kappa^6 + \frac{1}{\kappa^6}\right) = 0. \tag{33}$$

Equation (33) determines the width of the DB, $\kappa = e^{-q} = 0.8$. Having found the DB width, Eq. (31) and (32) are then solved to obtain the DB frequency $\omega^2 = 0.58\,918$ and the shape parameter of the chain $\mu = -0.102\,705$. In Fig. 6 we plot the variation of the angular difference $\beta = (\theta_{n+1} - \theta_{n-1})$ with each lattice site n. It depicts the chain curvature for which the system supports the DB solution of width and frequency as obtained above for arbitrary values of α (amplitude of the central site) and γ. It is appropriate to mention here that for Eq. (29) the even-parity mode ($\phi_n = -\phi_{-n}$) yields the same results as the odd-parity mode as shown above.

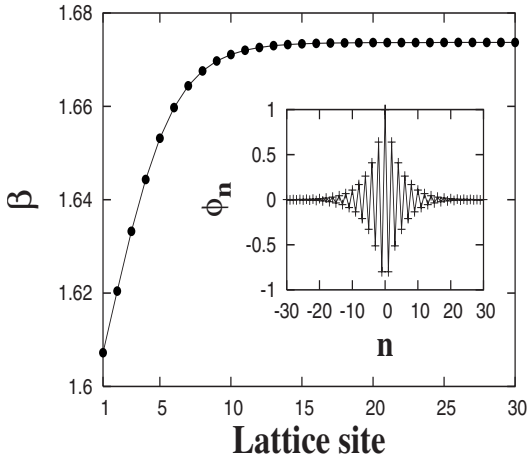

FIG. 6. Variation of the angular difference with lattice sites. Parameter values: $\alpha = 1.0$, $\gamma_1 = 1.0$. Inset: Spatial profile of the odd-parity DB mode of width, $\kappa = 0.8$ for the same parameter values.

IV. MOVING DISCRETE BREATHER

We now consider the case when θ_n are time dependent for all n. Here we seek moving DB solutions of the coupled equations of motion [Eqs. (10) and (11)]. For large breather amplitude and small angular differences between the adjacent lattice sites Eq. (10) and Eq. (11) are approximated, respectively, as

$$\ddot{\tau}_n - \tau_n\dot{\theta}_n^2 = g_{n+1} + g_{n-1} - 2g_n \tag{34}$$

and

$$\tau_n\ddot{\theta}_n + 2\dot{\tau}_n\dot{\theta}_n = g_{n+1}(\theta_{n+1} - \theta_n) + g_{n-1}(\theta_{n-1} - \theta_n). \tag{35}$$

We use the ansatz

$$\tau_n(t) = \psi_n(t)\cos(\omega t) \tag{36}$$

for the DB modes and define the angles $\theta_n(t) = \eta\,\psi_n(t)$, where η determines the shape of the chain. Using RWA we get an equation in $\psi_n(t)$ as

$$(2 + \eta^2\psi_n^2)\left(\frac{\partial\psi_n}{\partial t}\right)^2 + (\omega^2 - 2)\psi_n^2 + \frac{3}{2}\gamma\psi_n^4 = \frac{3}{4}\gamma(\psi_{n+1}^4 + \psi_{n-1}^4) - \frac{3}{2}\gamma\psi_n(\psi_{n+1}^3 + \psi_{n-1}^3) + (\psi_{n+1}^2 + \psi_{n-1}^2) - 2\psi_n(\psi_{n+1} + \psi_{n-1}) \tag{37}$$

Since we are interested in a solution that propagates with permanent shape and velocity, we write

$$\psi_n(t) = \psi(n - vt) = \psi(z), \quad z = n - vt, \tag{38}$$

where v is the velocity of the traveling discrete breather. Equation (38) converts Eq. (37) into an exactly similar equation in $\psi(z)$. We set the lattice constant $a = 1$ for simplicity.

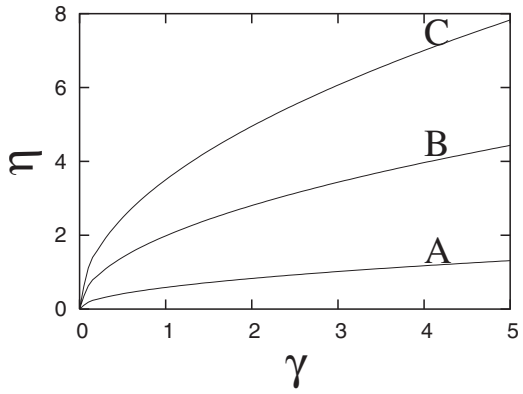

FIG. 7. Curvature versus anharmonicity for unit velocity. Curve A: $q=0.5$, $\omega=0.275$; curve B: $q=0.75$, $\omega=0.633$; curve C: $q=1.0$, $\omega=1.163$.

We look for a discrete exponentially localized solution $\psi(z)=A\ e^{-q|z|}$, where $q(>0)$ determines the DB width and A the DB amplitude. Substituting this in Eq. (37), written in terms of $\psi(z)$, and equating the coefficients of two different exponential terms to zero, we obtain two algebraic equations,

$$\omega^2 = 2 - 4\cosh(q) + 2\cosh(2q) - 2q^2v^2, \tag{39}$$

$$v^2 = \frac{3\gamma}{2\eta^2 q^2}[1 - 2\cosh(3q) + \cosh(4q)], \tag{40}$$

from which we obtain the velocity, frequency, and width of the DB for different values of η and γ. The allowed values of the parameters η and γ for which DB solutions exist are obtained from the real valuedness conditions of ω and v [Eq. (39) and Eq. (40)]. This is shown in Fig. 7 where the relation between parameters η and γ is plotted for three different DBs. The figure shows that with increase of the strength of anharmonicity γ, the bending of the chain should increase to support DBs of larger width and higher frequency.

Figure 8 demonstrates the trajectory of the moving discrete localized mode of an allowed width and velocity. Plots of the displacement pattern versus time at three different sites are laid down to illustrate how the oscillators in the curved chain respond as the excitation passes through the chain, and it depicts that the velocity of the excitation packet

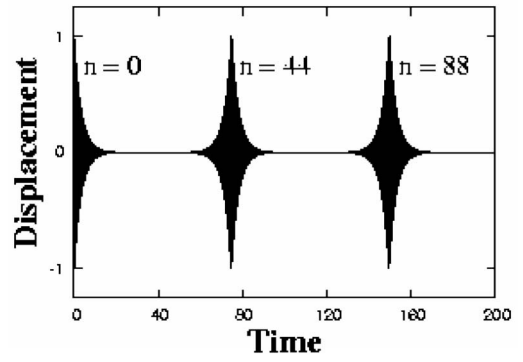

FIG. 8. Localized excitation passing three different lattice sites as a function of time. Values used: $q=0.5$, $\gamma=1$, $\eta=1$.

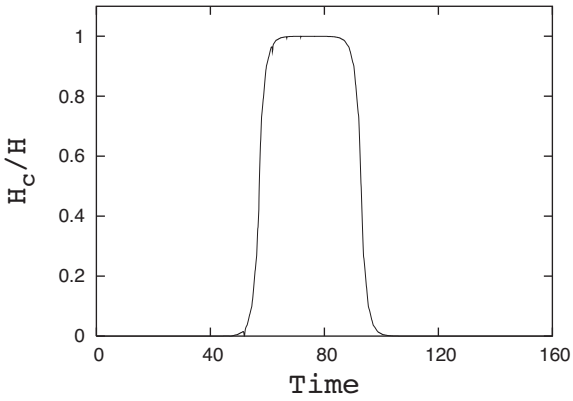

FIG. 9. Relative central energy H_c/H vs time.

remains a constant. This gives an important result that it is possible for a DB to travel through the FPU chain of a given shape with a constant velocity.

We also show that for a DB of an allowed width, all the energy can be transmitted along the curved FPU chain. According to Eqs. (1) and (3) and subsequent variable changes made, the potential and kinetic energies, respectively, are

$$V_n = \frac{K_2a^2}{2}\tau_n^2 + \frac{K_4a^4}{4}\tau_n^4$$

and

$$T_n = \tfrac{1}{2}(\dot{x}_n^2 + \dot{y}_n^2),$$

where $\dot{x}_n$ and $\dot{y}_n$ are computed according to

$$\dot{x}_n = \dot{x}_{n-1} + a\dot{\tau}_n\cos(\theta_n) - a(\tau_n + 1)\dot{\theta}_n\sin(\theta_n)$$

and

$$\dot{y}_n = \dot{y}_{n-1} + a\dot{\tau}_n\sin(\theta_n) + a(\tau_n + 1)\dot{\theta}_n\cos(\theta_n).$$

The Hamiltonian density is

$$H_n = T_n + V_n. \tag{41}$$

We use Eq. (41) to calculate the total DB energy $H=\Sigma_{n=0}^{N}H_n$ on a chain of $N=300$ sites. We also calculate the central energy $H_c=\Sigma_{n=34}^{54}$ in 21 sites around $n=44$ (the parameter values are used in Fig. 8). In Fig. 9 we plot the relative energy H_c/H as a function of time which shows that all the energy can be transmitted along the curved chain. The DB motion is practically lossless and determined through local energy conservation.

V. LONG-RANGE NONLINEAR DISPERSIVE INTERACTIONS

We now consider the question of existence of the ILMs in the curved FPU chain in the presence of long-range nonlinear dispersive interactions. Physical systems such as ionic and molecular crystals, polymers, biopolymers, such as proteins, contain various charged groups which interact through long-range Coulomb force. Additionally, excitation transfer in molecular crystals and energy transport in biopolymers are

due to transition dipole-dipole interaction [7,31]. There have been several studies of solitons and DBs in the presence of long-range interactions in one-dimensional chains [32]. There are a few cases where the dynamics of the curved chain in the presence of long-range interactions are considered, but the geometry of the chain is restricted to a fixed simple one such as hairpin, parabolic, wedge shaped, etc. [23,21,22]. In the presence of long-range interactions, the geometry of the chain becomes very relevant as the distance between the units in the chain changes and therefore the intensity of the coupling between them. We therefore study the more general problem by considering the arbitrary shape of the chain which may be fixed or change with time and by introducing long-range interactions in terms of two long-range interaction parameters s_1 and s_2 characterizing the harmonic and anharmonic long-range dispersive interactions, respectively. The Hamiltonian is given by

$$H = \sum_n \left(\frac{\dot{x}_n^2}{2} + \frac{\dot{y}_n^2}{2} + V \right), \tag{42}$$

where the long-range interaction potential V is assumed to have power dependence r^{-s} on the distance given by

$$V = \sum_p \left(\frac{K_2}{2} \frac{(d_{n,p} - a)^2}{|p|^{s_1}} + \frac{K_4}{4} \frac{(d_{n,p} - a)^4}{|p|^{s_2}} \right) \tag{43}$$

and

$$d_{n,p} = [(x_n - x_{n-p})^2 + (y_n - y_{n-p})^2]^{1/2}, \quad p = 1,2,3, \ldots .$$

The corresponding equations of motion are

$$\ddot{\tau}_n - (\tau_n + 1)\dot{\theta}_n^2 = \sum_p [g_{n+p,p} \cos(\theta_{n+p} - \theta_n) + g_{n-p,p} \cos(\theta_{n-p} - \theta_n) - 2g_{n,p}], \tag{44}$$

$$(\tau_n + 1)\ddot{\theta}_n + 2\dot{\tau}_n\dot{\theta}_n = \sum_p [g_{n+p,p} \times \sin(\theta_{n+p} - \theta_n) + g_{n-p,p} \sin(\theta_{n-p} - \theta_n)], \tag{45}$$

where, $g_{n,p} = \frac{\tau_n}{|p|^{s_1}} + \gamma \frac{\tau_n^3}{|p|^{s_2}}$. For $p=1$ (nearest-neighbor interaction), these equations reduce to Eqs. (10) and (11), respectively. It is a very difficult problem to solve these coupled, discrete nonlinear differential equations [Eqs. (44) and (45)] analytically. For the case of harmonic interaction between oscillators, analytic solutions can be obtained by approximate methods like the variational method and lattice Green's function method. Such methods cannot be implemented as easily in the present case with anharmonic nonlocal dispersive interactions. However, we realized that the exponential discrete breathers in which we are interested here can be obtained analytically up to the second-neighbor interaction in the chain. This enables us to compare the localization properties of the DB solutions for nearest-neighbor and next-nearest-neighbor cases. These are discussed in the following section (Sec. V A). Similar calculations for long-range interactions up to second-neighbor coupling are also reported in [23]. For all neighbors interactions, we treat the problem in the continuum limit which is discussed in the next section (Sec. V B).

A. First- and second-neighbor interactions

An analysis similar to that in Sec. III ($p=1$ case) can be carried out considering the second-neighbor interactions ($p=1$ and 2). As in Sec. III, we first consider only Eq. (44) with time independent θ_n for the dynamics of the curved FPU chain. Equation (44) (with $\dot{\theta}_n = 0$ for all n) is equivalent to Eq. 8 in [20] but with long-range interactions. The dynamics of the coupled equations (44) and (45) with long-range interactions and time dependent θ_n follows in the next section. Taking into account the first two terms in the summation ($p=1,2$) in Eq. (44) with $\dot{\theta}_n = 0$, we obtain the dynamical equation as

$$\ddot{\tau}_n = g_{n+1} \cos(\theta_{n+1} - \theta_n) + g_{n-1} \cos(\theta_{n-1} - \theta_n) + g_{n+2,2} \cos(\theta_{n+2} - \theta_n) + g_{n-2,2} \cos(\theta_{n-2} - \theta_n) - 2(g_n + g_{n,2}). \tag{46}$$

We look for static DB solutions of the form of Eq. (14) to this equation. We define the geometry of the chain in terms of the second-neighbor angular deviations as

$$\cos(\theta_{n+2} - \theta_n) = \frac{\mu}{(1 + 2^{s_1 - s_2}\gamma_1 \phi_{n+2}^2)},$$

$$\cos(\theta_{n-2} - \theta_n) = \frac{\mu}{(1 + 2^{s_1 - s_2}\gamma_1 \phi_{n-2}^2)}, \tag{47}$$

where $s_2 < s_1$ and the nearest-neighbor angular deviations are taken as in Eq. (15). Using RWA, the equation for DB solutions and using RWA, the equation for ϕ_n thus derived from Eq. (46) is

$$-\omega^2 \phi_n = \mu\phi_{n+1} + \mu\phi_{n-1} + \frac{\mu}{2^{s_1}}\phi_{n+2} + \frac{\mu}{2^{s_1}}\phi_{n-2} - 2\left(1 + \frac{1}{2^{s_1}}\right)\phi_n - 2\left(1 + \frac{1}{2^{s_2}}\right)\gamma_1 \phi_n^3 \tag{48}$$

As in Sec. III, we obtain the homogeneous plane wave solutions by ignoring the quartic term in the potential [Eq. (43)] and derive the dispersion relation

$$\omega^2 = 2\left(1 + \frac{1}{2^{s_1}}\right) - 2\mu\left(\cos(q) + \frac{1}{2^{s_1}}\cos(2q)\right), \tag{49}$$

where the real wave vector is given by $q = (2j+1)\pi$, j being an integer. The maximum plane wave frequency in this case is $\omega_m^2 = 2\left[\left(1 + \frac{1}{2^{s_1}}\right) + \mu\left(1 - \frac{1}{2^{s_1}}\right)\right]$ and the inhomogeneous wave solutions characterized by a complex wave vector $q^* = q \pm iq'$ have frequencies larger than this. We look for odd-parity solutions of the form of Eq. (20) with $\phi_0 = \alpha$. From Eq. (48) we obtain the equations for $n=0$ and $n=1$, respectively, as

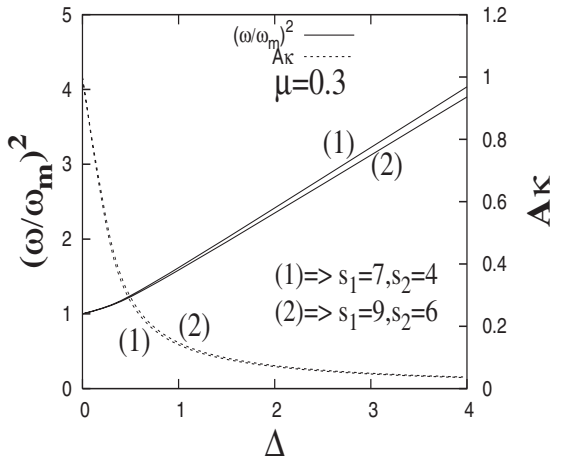

FIG. 10. Local-mode frequency and relative amplitude versus anharmonicity for two sets of the long-range interaction parameters s_1 and s_2.

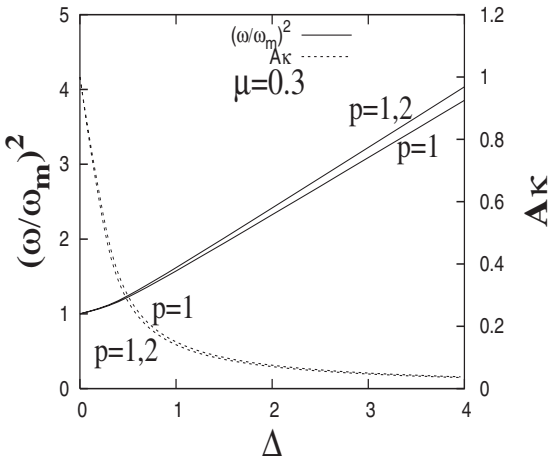

FIG. 11. Local-mode frequency and relative amplitude versus anharmonicity with nearest- and second-nearest neighbor ($s_1=7$, $s_2=4$) interactions.

$$\left(\frac{\omega}{\omega_m}\right)^2 = \frac{\left(1+\frac{1}{2^{s_1}}\right)+\Delta\left(1+\frac{1}{2^{s_2}}\right)+\mu A\kappa\left(1-\frac{\kappa}{2^{s_1}}\right)}{\left(1+\frac{1}{2^{s_1}}\right)+\mu\left(1-\frac{1}{2^{s_1}}\right)} \tag{50}$$

and

$$\left(\frac{\omega}{\omega_m}\right)^2 = \frac{1}{2\left[\left(1+\frac{1}{2^{s_1}}\right)+\mu\left(1-\frac{1}{2^{s_1}}\right)\right]}\left[2\left(1+\frac{1}{2^{s_1}}\right)+\mu\left(\kappa+\frac{1}{A\kappa}\right)+2\Delta A^2\kappa^2\left(1+\frac{1}{2^{s_2}}\right)-\frac{\mu}{2^{s_1}}(1+\kappa^2)\right] \tag{51}$$

Following the same procedure of obtaining the dispersion relation for the localized modes [Eq. (19)] with nearest-neighbor interactions, we obtain the local-mode dispersion relation with next-nearest-neighbor interactions in terms of κ and the maximum harmonic frequency ω_m as

$$\left(\frac{\omega}{\omega_m}\right)^2 = \frac{2\left(1+\frac{1}{2^{s_1}}\right)+\mu\left(\kappa+\frac{1}{\kappa}\right)-\frac{\mu}{2^{s_1}}\left(\kappa^2+\frac{1}{\kappa^2}\right)}{2\left[\left(1+\frac{1}{2^{s_1}}\right)+\mu\left(1-\frac{1}{2^{s_1}}\right)\right]}. \tag{52}$$

Solving Eqs. (50)–(52) simultaneously we get the frequency, amplitude, and width of the ILM for given values of anharmonicity Δ, chain curvature μ and arbitrary values of the long-range parameters s_1 and s_2. Figure 10 gives a typical example of the calculated DB frequencies and relative amplitudes as functions of Δ for a given curvature ($\mu=0.3$) of the chain and two particular sets of the long-range parameters. As the values of s_1 and s_2 decrease, the amplitudes of the neighbors decrease with respect to that of the central site thereby implying higher localization of the DB mode while the DB frequency increases.

A simple approximate description of the long-range dipole-dipole-like interactions can also be accounted for using this model for choice of the parameter values $s_1=3$ and $s_2=0$. In such a case discrete breathers still exist but for lower Δ values. DBs also exist for $s_1=3$ and $s_2=1$, $s_2=2$. Figures 11 and 12 compare the results of next-nearest-neighbor ($p=1,2$) interactions with that of the nearest-neighbor interaction ($p=1$) case. With the introduction of the second-neighbor ($p=1,2$) interactions in the given bent chain, the DB frequency increases while the relative amplitude decreases, thus making the DB mode more localized. This is shown in Fig. 11. In Fig. 12 we plot the nearest-neighbor angular deviations $(\theta_{n+1}-\theta_n)$ as functions of the lattice sites. With the inclusion of the second-neighbor interactions in the curved FPU chain the angular deviations decrease which therefore implies that less curvature of the chain is required for DB excitations.

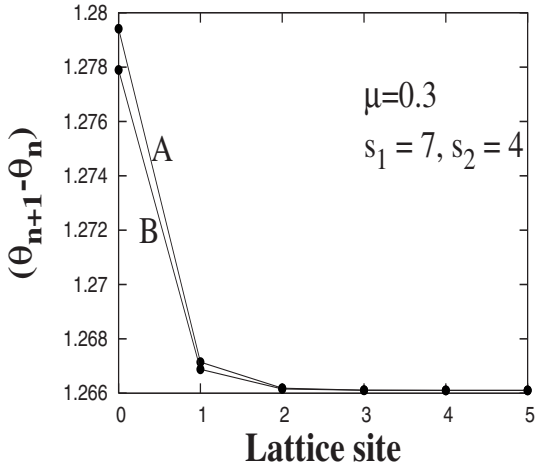

FIG. 12. Change of the angular deviations between the nearest neighbors with lattice sites for $\Delta=0.5$. Curve A: $p=1$; curve B: $p=1,2$.

B. The continuum limit

The analytic calculations become increasingly difficult with more number of neighbors interacting (for $p>2$) in the bent chain and one must resort to numerical calculations. However, in the presence of long-range interactions, some of the spatially localized solutions that we are looking for can be obtained in the continuum limit. The advantage of obtaining the continuum solutions is that it may be useful to use these solutions as initial conditions for obtaining the solutions of the actual discrete lattice equations numerically. The corresponding equation of motion [Eq. (46)] in the weakly nonlinear limit is given by

$$\tau_{tt} = \zeta(s_1-2)\tau_{xx} + \tfrac{1}{12}\zeta(s_1-4)\tau_{xxxx} + \gamma\zeta(s_2-2)(\tau^3)_{xx} - \left[\tfrac{1}{2}\zeta(s_1-4)\tau_{xx} + \tfrac{1}{2}\gamma\zeta(s_2-4)(\tau^3)_{xx} + \gamma\zeta(s_2-2)\tau^3 + \zeta(s_1-2)\tau\right]\theta_x^2, \tag{53}$$

where subscripts denote partial derivatives and $\zeta(s)$ is the Reimann zeta function [33]. This equation supports static breather solutions of the form $\tau(x,t)=y(x)\cos(\omega t)$, where $y(x)=A\tanh(Bx)$, long-range parameters being $s_2=2$, $s_1>5$ and time-independent shape of the chain is defined by $\theta_x = \eta y(x)$.

For traveling wave solutions with long-range interactions, we consider both the coupled equations of motion [Eqs. (44) and (45)] in the long-wavelength limit where we take into account the time dependence of the site angles θ_n for all n. In the weakly nonlinear and large amplitude limit the corresponding dynamical equations, respectively, are

$$\tau_{tt} - \tau\theta_t^2 = \zeta(s_1-2)\tau_{xx} + \tfrac{1}{12}\zeta(s_1-4)\tau_{xxxx} + \gamma\zeta(s_2-2)(\tau^3)_{xx} - \left[\tfrac{1}{2}\zeta(s_1-4)\tau_{xx} + \tfrac{1}{2}\gamma\zeta(s_2-4)(\tau^3)_{xx} + \gamma\zeta(s_2-2)\tau^3 + \zeta(s_1-2)\tau\right]\theta_x^2 \tag{54}$$

and

$$\tau\theta_{tt} + 2\theta_t\tau_t = \left[6\gamma\zeta(s_2-2)\tau^2\tau_x + \tfrac{1}{3}\zeta(s_1-4)\tau_{xxx} + 2\zeta(s_1-2)\tau_x\right]\theta_x. \tag{55}$$

We consider the time-dependent shape of the chain as $\theta(x,t)=\mu\tanh[B(x-vt)]$. It can be easily shown that the above equations support traveling soliton solutions of the form

$$\tau(x,t) = A\tanh[B(x-vt)], \tag{56}$$

where the velocity, amplitude, and width of the kink are, respectively, given by

$$v^2 = \frac{7}{8}\zeta(s_1-2), \quad A^2 = \frac{\zeta(s_1-2)}{\gamma}, \quad B^2 = \frac{3\zeta(s_1-2)}{8\zeta(s_1-4)}$$

for the shape parameter $\mu=\pm 3$, long-range interaction parameters $s_2=2$, $s_1>5$ and the anharmonicity parameter $\gamma>0$. The allowed range of the long-range interaction parameters is determined from the finiteness condition of the Riemann zeta function and the real valuedness conditions of the amplitude, velocity, and width of the kink soliton. As can be seen from the expressions above, the kink moves in the curved chain with a subsonic velocity $\left(\frac{v}{c_0}\right)^2=\frac{7}{8}$, where $c_0^2=\zeta(s_1-2)$ is the characteristic velocity of linear (sound) waves in the chain. The kink amplitude and width depends on the kink velocity, which is the characteristic of a soliton solution. Such kink-soliton solutions have also been obtained earlier in the continuum limit of one-dimensional nonlinear lattices with long-range harmonic interactions [32]. It is worth mentioning here that these continuum coupled equations viz., Eqs. (54) and (55) also support traveling compact breather solutions [30].

VI. FINITE AMPLITUDE EXACT SINUSOIDAL WAVES

It is known that linear sinusoidal waves are low-lying excitations or phonon eigenmodes of the lattice. Similarly, it has been shown that for a one-dimensional FPU lattice it is possible to excite a nonlinear finite amplitude traveling or standing wave of exact sinusoidal displacement pattern with commensurate wave length $\lambda=3a$ or "magic" wave number $k=2\pi/3a$ (a is lattice constant) [34]. Exact extended propagating nonlinear sinusoidal waves (NSWs) having this particular wave number in the FPU and other nonlinear lattices have recently been found by others [35]. Contrary to the linear sinusoidal waves, the frequency of the NSWs depends on the amplitude, while the wave number is determined by the anharmonic interactions. The vibrational eigenstates of the anharmonic lattices can be expressed in terms of these exact NSWs and therefore, they contribute to the specific heat and energy transport in the systems. Hence, NSWs should be considered for a complete thermodynamic description of the anharmonic lattices. Here we show that NSWs are also exact solutions of the curved FPU chain. We look for solutions in the form of traveling sinusoidal waves

$$\tau_n = A\cos(kna-\omega t). \tag{57}$$

We determine the amplitude-dependent frequency ω and allowed wave numbers k for which such NSWs exist. We find that the coupled equation of motion Eq. (28) admits NSW solutions of the form of Eq. (57) for the time-independent geometry of the chain given by the relation $\cos(\theta_{n+1}-\theta_{n-1})=1$ for two allowed short commensurate wave numbers, one of which is the "magic" wave number $ka=\frac{2\pi}{3}$ and the other $ka=\pi-\frac{2\pi}{3}=\frac{\pi}{3}$. The frequency of the NSW is given by $\omega^2=3+\frac{9}{4}\gamma A^2$, where the amplitude A is arbitrary.

NSWs can also be obtained when θ_n are time dependent for all n. In this case, we show that NSWs are exact solutions of the curved FPU chain with wave numbers (that depend on the shape of the chain) which are different from the "magic" wave number as predicted to exist in the corresponding one-dimensional FPU lattice [34,35]. We approximate the angular difference between the neighboring lattice sites to quadratic order and in the large amplitude limit the coupled equations (10) and (11), respectively, reduce to

$$\ddot{\tau}_n - \tau_n\dot{\theta}_n^2 = g_{n+1} + g_{n-1} - 2g_n - g_{n+1}\frac{(\theta_{n+1}-\theta_n)^2}{2} - g_{n-1}\frac{(\theta_{n-1}-\theta_n)^2}{2} \tag{58}$$

and

$$\tau_n\ddot{\theta}_n + 2\dot{\tau}_n\dot{\theta}_n = g_{n+1}(\theta_{n+1} - \theta_n) + g_{n-1}(\theta_{n-1} - \theta_n), \quad (59)$$

where $g_n = K_2\tau_n + K_4 a^2 \tau_n^3$. The above two equations can be combined to obtain a single difference-differential equation of the form

$$\frac{\partial^2}{\partial t^2}(\tau_n\theta_n) - \tau_n\theta_n\left(\frac{\partial\theta_n}{\partial t}\right)^2 = g_{n+1}\theta_{n+1} + g_{n-1}\theta_{n-1} - [g_{n+1}(\theta_{n+1} - \theta_n)^2 + g_{n-1}(\theta_{n-1} - \theta_n)^2 + 4g_n]\frac{\theta_n}{2}. \quad (60)$$

We consider the time-dependent shape of the chain of the form $\theta_n(t) = \eta\cos(kna - \omega t)$. In this case, Eq. (60) supports NSW solutions of the form of Eq. (57) for two different short incommensurate wave numbers $ka = \frac{7\pi}{8}$ and $ka = \frac{3\pi}{8}$. For $k = \frac{7\pi}{8a}$, $\eta^2 = 2.9$, and the NSW frequency and amplitude are, respectively, given by

$$\omega^2 = 0.12K_2, \quad A^2 = \frac{1.24K_2}{|K_4|a^2},$$

where the quartic anharmonic strength $K_4 < 0$ and harmonic strength $K_2 > 0$. Thus, we see that for a given value of K_2, the NSW amplitude decreases as the magnitude of the anharmonicity in the chain increases. For the other allowed wave number $k = \frac{3\pi}{8a}$, $\eta^2 = 7$, and the NSW frequency and amplitude, respectively, are

$$\omega^2 = 0.29|K_2|, \quad A^2 = \frac{1.57|K_2|}{K_4 a^2}$$

for $K_4 > 0$ and $K_2 < 0$.

We have obtained the NSW solutions for a parabolic shape of the FPU chain as well. We substitute $y_n = \frac{\eta}{2}x_n^2$ in the coupled equations of motion, Eqs. (4) and (5), where η is the shape parameter to obtain the dynamical equation for $x_n(t)$ as

$$\begin{aligned}\dot{x}_n^2 = {} & \tfrac{1}{4}K_4\eta^2 x_n^6 + \tfrac{1}{2}K_2(x_{n+1}^2 + x_{n-1}^2) + \tfrac{1}{2}K_4(x_{n+1}^4 + x_{n-1}^4) \\ & + \tfrac{1}{8}K_4\eta^2(x_{n+1}^6 + x_{n-1}^6) + x_n^2\big[K_2 + 3K_4(x_{n+1}^2 + x_{n-1}^2) \\ & - \tfrac{1}{8}K_4\eta^2(x_{n+1}^4 + x_{n-1}^4)\big] - x_n\big[K_2(x_{n+1} + x_{n-1}) + 2K_4(x_{n+1}^3 \\ & + x_{n-1}^3) + \tfrac{1}{4}K_4\eta^2(x_{n+1}^5 + x_{n-1}^5)\big] - 2K_4x_n^3\big[(x_{n+1} + x_{n-1}) \\ & - \tfrac{1}{4}\eta^2(x_{n+1}^3 + x_{n-1}^3)\big] - K_4x_n^4\big[1 - \tfrac{1}{8}\eta^2(x_{n+1}^2 + x_{n-1}^2)\big] \\ & - \tfrac{1}{4}K_4\eta^2x_n^5(x_{n+1} + x_{n-1}). \end{aligned} \quad (61)$$

This equation supports NSW solutions of the form of Eq. (57) viz., $x_n = A\cos(kna - \omega t)$ for two allowed short wave numbers, one of which is commensurate with the lattice $k = \pm\frac{\pi}{6a}$ and the other incommensurate $k = \pm\frac{5\pi}{6a}$. For $k = \pm\frac{\pi}{6a}$, $\eta^2 = \frac{0.11K_4}{|K_2|}$, and the NSW frequency and amplitude are, respectively,

$$\omega^2 = 1.128|K_2|, \quad A^2 = \frac{19.44|K_2|}{K_4}, \quad (62)$$

where $K_2 < 0$ and $K_4 > 0$. The velocity of this particular NSW excitation is $V = \frac{\omega}{\pi/6}$ (taking $a = 1$) which turns out to be supersonic. For $k = \pm\frac{5\pi}{6a}$, the frequency and amplitude of the corresponding NSW are, respectively, given by

$$\omega^2 = 0.2K_2, \quad A^2 = \frac{0.25K_2}{|K_4|}, \quad (63)$$

for $K_2 > 0$, $K_4 < 0$ and the shape parameter $\eta^2 = \frac{118|K_4|}{K_2}$. This is a subsonic NSW. From the expressions above, we find that the velocity of the NSW varies directly with its amplitude. This is in agreement with earlier studies of NSW in FPU and Lennard-Jones anharmonic lattices in one-spatial dimension [36]. From Eqs. (62) and (63) it can be seen that for given values of harmonic and anharmonic interaction strengths K_2 and K_4, respectively, the velocity as well as the amplitude of the NSWs decrease with increasing chain curvature.

VII. CONCLUSION

In this paper we have explored the nature of localized modes in a curved FPU chain and the effect of geometry, long-range interactions, and nonlinear dispersion on the localization and movability properties of these modes. We have shown that exponential, static DBs are exact solutions of the corresponding discrete equations of motion for chosen geometries of the system. The nature of localization of the modes depends on the anharmonicity and the curvature of the chain. For lower anharmonicity of the chain the modes are delocalized. For higher anharmonicity the modes are localized and the extent of localization depends on the chain geometry. It is seen that the local-mode frequency increases with increasing anharmonicity. The results for the even DB modes are qualitatively similar to those for the odd DB modes. However, a quantitative difference is that for a given anharmonicity and curvature of the chain, the even mode is more localized than the odd mode and the frequency of the even mode is higher than that of the odd mode. We also show that purely anharmonic short-range interaction potential gives rise to exact compactlike discrete breathers in the system. While the amplitude of such compactlike localized modes is characteristically independent of the width, it varies with the anharmonicity in the chain. In the strong anharmonic limit there is almost no significant change in the amplitudes of the compactlike DBs for a given curvature of the chain.

The curved chain of nonlinear oscillators interacting through an FPU-type potential also admits large amplitude moving DB solutions. The interplay of curvature and nonlinearity effects the DB velocity and frequency. We have shown that a moving DB excitation of an allowed width (as determined by the curvature of the chain) can pass through the curved chain with constant velocity.

We have also analyzed the spatial localization properties and movability of the DBs in the presence of long-range nonlinear dispersive interactions. We have obtained the exact static DB solutions of the curved discrete FPU lattice by considering up to the second-neighbor coupling for a given geometry. Comparison of the results with that obtained for the nearest-neighbor interaction shows that the introduction of the next-nearest-neighbor interactions in the chain decreases the relative amplitudes thus making the DB modes

more localized and their excitation is more favorable in a chain with lower curvature. Using the continuum limit approximation, we have shown the existence of static breather solutions as well as traveling kink-soliton solutions which move with subsonic velocity in the curved chain for all neighbors interactions.

We further show that exact traveling nonlinear sinusoidal waves with short commensurate and incommensurate wavelengths and in general, amplitude-dependent frequency are exact solutions of the dynamical equations of the curved FPU chain for its different geometries. The existence of NSWs influences the classification of the large-amplitude vibrational eigenstates and therefore, they must be considered for a complete thermodynamic description of the anharmonic lattices.

ACKNOWLEDGMENTS

The authors would like to thank DST (India) for financial assistance through a research grant. One of the authors (B.D.) would like to thank G.P. Tsironis for discussions.

[1] B. I. Swanson, J. A. Brozik, S. P. Love, G. F. Strouse, A. P. Shreve, A. R. Bishop, W. Z. Wang, and M. I. Salkola, Phys. Rev. Lett. **82**, 3288 (1999).
[2] U. T. Schwarz, L. Q. English, and A. J. Sievers, Phys. Rev. Lett. **83**, 223 (1999).
[3] A. Ustinov, Chaos **13**, 716 (2003).
[4] J. W. Fleischer, M. Segev, N. K. Efremidis, and D. N. Christodoulides, Nature (London) **422**, 147 (2003).
[5] C. M. Soukoulis, *Photonic Crystals and Light Localization in the 21st Century*, NATO Science Series C 563 (Kluwer Academic, Dordrecht, Boston, London, 2001).
[6] F. M. Russell and J. C. Eilbeck, Europhys. Lett. **78**, 10004 (2007).
[7] *Nonlinear Excitations in Biomolecules*, edited by M. Peyrard (Springer, Berlin, 1995); L. V. Yakushevich, *Nonlinear Physics of DNA*, (Wiley, New York, 1998); A. Scott, *Nonlinear Science: Emergence and Dynamics of Coherent Structures*, 2nd ed. (Oxford University Press, Oxford, 2003).
[8] A. J. Heeger *et al.*, Rev. Mod. Phys. **60**, 781 (1988).
[9] N. Lazarides, M. Eleftheriou, and G. P. Tsironis, Phys. Rev. Lett. **97**, 157406 (2006).
[10] D. K. Campbell, S. Flach, and Y. S. Kivshar, Phys. Today **57** (1), 43 (2004); see also, Chaos **13**, 586 (2003).
[11] J. L. Marin, J. C. Eilbeck, and F. M. Russel, *Nonlinear Science at the Dawn of the 21st Century*, edited by P. L. Christiansen and M. P. Soerensen (Springer, Berlin, 2000).
[12] D. Chen, S. Aubry, and G. P. Tsironis, Phys. Rev. Lett. **77**, 4776 (1996); M. Peyrard, Physica D **119**, 184 (1998).
[13] R. Mohr, K. Kratz, T. Weigel, M. Lucks-Gabor, M. Moneke, and A. Lendlein, Proc. Natl. Acad. Sci. U.S.A. **103**, 3540 (2006).
[14] S. Takeno, J. Phys. Soc. Jpn. **59**, 1571 (1990); S. Takeno, *ibid.* **61**, 28211 (1992).
[15] J. M. Tamga, M. Remoissenet, and J. Pouget, Phys. Rev. Lett. **75**, 357 (1994).
[16] I. A. Butt and J. A. D. Wattis, J. Phys. A **39**, 4955 (2006).
[17] D. Bonart, A. P. Mayer, and U. Schroder, Phys. Rev. B **51**, 13739 (1995); V. M. Burlakov, S. A. Kiselev, and V. N. Pyrkov, *ibid.* **42**, 4921 (1990).
[18] J. J. Mazo, Phys. Rev. Lett. **89**, 234101 (2002).
[19] J. Gomez-Gardenes, L. M. Floria, and A. R. Bishop, Physica D **216**, 31 (2006).
[20] G. P. Tsironis, M. Ibanes, and J. M. Sancho, Europhys. Lett. **57**, 697 (2002).
[21] P. V. Larsen, P. L. Christiansen, O. Bang, J. F. R. Archilla, and Yu. B. Gaididei, Phys. Rev. E **70**, 036609 (2004).
[22] P. V. Larsen, P. L. Christiansen, O. Bang, J. F. R. Archilla, and Yu. B. Gaididei, Phys. Rev. E **69**, 026603 (2004).
[23] M. Ibanes, J. M. Sancho, and G. P. Tsironis, Phys. Rev. E **65**, 041902 (2002).
[24] J. L. Marin, J. C. Eilbeck, and F. M. Russel, Phys. Lett. A **248**, 225 (1998); **281**, 21 (2001).
[25] S. R. Bickham and A. J. Sievers, Phys. Rev. B **43**, 2339 (1991); S. R. Bickham, A. J. Sievers, and S. Takeno, *ibid.* **45**, 10344 (1992).
[26] P. Rosenau and S. Shochet, Chaos **15**, 015111 (2005), and references therein; B. Dey, Phys. Rev. E **57**, 4733 (1998); B. Dey and A. Khare, Phys. Rev. E **58**, R2741 (1998).
[27] M. Eleftheriou, B. Dey, and G. P. Tsironis, Phys. Rev. E **62**, 7540 (2000).
[28] B. Dey, M. Eleftheriou, S. Flach, and G. P. Tsironis, Phys. Rev. E **65**, 017601 (2001).
[29] A. V. Gorbach and S. Flach, Phys. Rev. E **72**, 056607 (2005).
[30] R. Sarkar and B. Dey, J. Phys. A **39**, L99 (2006).
[31] A. S. Davydov, *Theory of Molecular Excitons* (Plenum, New York, 1971); A. C. Scott, Phys. Rep. **217**, 1 (1992).
[32] A. Neuper *et al.*, Phys. Lett. A **190**, 165 (1994); P. Woafo, T. C. Kofane, and A. S. Bokosah, Phys. Rev. B **48**, 10153 (1993); C. T. Kamga and T. C. Kofane, Phys. Rev. E **50**, 2257 (1994); N. Gronbech-Jensen and M. R. Samuelsen, Phys. Rev. Lett. **74**, 170 (1995); Y. Gaididei *et al.*, Physica D **107**, 83 (1997), and references therein; K. O. Rasmussen *et al.*, Physica D **113**, 134 (1998); D. Bonart, *ibid.* **231**, 201 (1997).
[33] B. Dey, M. Eleftheriou, and G. P. Tsironis, in *Nonlinearity and Disorder: Theory and Applications*, edited by F. Abdullaev *et al.*, (Kluwer, Dordrecht, 2001), pp. 189–195.
[34] Y. A. Kosevich, Phys. Rev. Lett. **71**, 2058 (1993); M. Rodriguez-Achach and G. Perez, *ibid.* **79**, 4715 (1997).
[35] B. Rink, Physica D **175**, 31 (2003); G. M. Chechin, N. V. Novikova, and A. A. Abramenko, *ibid.* **166**, 208 (2002); S. Shinohara, J. Phys. Soc. Jpn. **71**, 1802 (2002); P. Poggi and S. Ruffo, Physica D **103**, 251 (1997).
[36] Y. A. Kosevich, R. Khomeriki, and S. Ruffo, Europhys. Lett. **66**, 21 (2004).